

# Negative-Parity States and $\beta$ -decays in odd Ho and Dy Nuclei with A=151,153

Falih H. Al-Khudair<sup>1,2</sup>, Gui Lu Long<sup>1,2</sup> and Yang Sun<sup>3</sup>

<sup>1</sup>Department of Physics, Tsinghua University, Beijing 100084, China

<sup>2</sup>Center of Nuclear Theory, Lanzhou Heavy Ion National Laboratory, Lanzhou, 730000, China

<sup>3</sup>Department of Physics, Shanghai JiaoTong University, Shanghai 200240, China

(Dated: 2007-12-18)

We have investigated the negative-parity states and electromagnetic transitions in <sup>151,153</sup>Ho and <sup>151,153</sup>Dy within the framework of the interacting boson fermion model 2 (IBFM-2). Spin assignments for some states with uncertain spin are made based on this calculation. Calculated excitation energies, electromagnetic transitions and branching ratios are compared with available experimental data and a good agreement is obtained. The model wave functions have been used to study  $\beta$ -decays from Ho to Dy isotones, and the calculated  $\log ft$  values are close to the experimental data.

PACS numbers: 21.60.Fw, 23.40.Hc, 27.70.+q

## I. INTRODUCTION

The interacting boson model (IBM) has been remarkably successful in describing the collective phenomena observed in even-even medium to heavy mass nuclei [1, 2, 3]. In the simplest version of this model, the IBM-1, the nuclear properties are described by a system of a fixed number of boson. In this version no distinction is made between proton boson and neutron boson, therefore all states in IBM-1 are  $F$ -spin symmetric [4, 5, 6]. The building blocks are  $(s^\dagger, \bar{s})$  for s-boson and  $(d^\dagger, \bar{d})$  for d-boson. The second version, the IBM-2, does distinguish between proton boson and neutron boson. The states in IBM-2 include all the  $F$ -spin symmetric states as well as mixed symmetry states belonging to the U(6) representation  $[N-1, 1]$ . An important property of this new version is that the proton - neutron symmetry character of each state is specified in terms of a new quantum number called  $F$ -spin [7, 8, 9, 10, 11]. For lighter nuclei, the IBM has been extended to the interacting boson model with isospin (IBM-3) [12]. Within the IBM-3, the neutron-proton pair must be included in addition to the two other types of bosons in the IBM-2, and they form an isospin triplet [13, 14, 15, 16, 17]. In the interacting boson fermion model (IBFM) [18], odd-A nuclei are described by coupling the degrees of freedom of odd particle to a core which is described in the IBM. Calculations of positive and negative-parity states and the electromagnetic transitions of odd mass nuclei have been performed within the framework of IBFM, for instance in Refs. [19, 20, 21, 22, 23, 24]. One of the most important properties in nuclear structure study is the  $\beta$  decay rates. The  $\beta$  transition for odd-nuclei has received intensive interests in the last few years [25, 26, 27, 28, 29, 30, 31, 32]. Theoretical contribution to the study of nuclear beta decay has been made over the years using the IBFM [33, 34, 35], and good agreement has been found with available experimental data.

The purpose of the present work is to investigate the negative-parity states and electromagnetic transitions in the <sup>151,153</sup>Ho and <sup>151,153</sup>Dy isotopes by using the IBFM-2 model. More importantly,  $\beta$  decay between the levels are studied by using the wave functions obtained from the structure calculation of this model. In particular, the influence of different values of hamiltonian parameters on the energies and decay probabilities is investigated.

In order to calculate an odd-nucleus in the IBFM-2 model, we need to choose an even-even core. Here, the even-even <sup>150,152</sup>Dy nuclei have been chosen as the respective core for <sup>151,153</sup>Dy isotopes. They have 66 protons in the 50 – 82 shell and 84 and 86 neutrons in shell 82 – 126, respectively. Both nucleons lie in the first half shell, therefore they should be considered as particle bosons. For <sup>151,153</sup>Ho isotopes, we considered them as resulting from coupling a proton hole to the even-even Er nuclei.

In section II, we briefly review the interacting boson fermion model. In section III, we present our calculation results for the energy levels of the core nuclei and compared with available data. The negative-parity states of <sup>151,153</sup>Ho and <sup>151,153</sup>Dy nuclei are presented in sections IV and V, respectively. A discussion of electromagnetic transitions follows in section VI. In section VII the  $\beta$  decay from levels of odd-proton Ho-isotopes to levels in odd-neutron Dy-isotopes levels are studied. Finally, in section VIII we summarize our results.

## II. THE IBFM-2 MODEL

The low lying levels in odd nuclei are described as combined system of a group of bosons with one fermion. In general, the Hamiltonian for this coupled system can be written as [34],

$$H = H_B + H_F + V_{BF}. \quad (1)$$

Here  $H_B$  is the usual IBM-2 Hamiltonian which describes the system of  $(s_\nu, s_\pi)$  and  $(d_\nu, d_\pi)$ -bosons

$$H = \varepsilon_d(\hat{n}_{d\pi} + \hat{n}_{d\nu}) + \kappa_{\pi\nu}\hat{Q}_\pi \cdot \hat{Q}_\nu + \sum_{\rho=\pi,\nu} \hat{V}_{\rho\rho} + \hat{M}_{\pi\nu}, \quad (2)$$

where  $\varepsilon_d$  is the d-boson excitation energy, and  $n_{d\pi}$  and  $n_{d\nu}$  are the neutron and proton d-boson number operator respectively.  $\kappa_{\pi\nu}\hat{Q}_\pi \cdot \hat{Q}_\nu$  is the quadruple interaction between proton and neutron boson, and  $\hat{Q}_\rho$ , the quadruple operator, is given by

$$\hat{Q}_\rho = (s_\rho^\dagger \tilde{d}_\rho + s^\dagger d_\rho^\dagger)^2 + \chi_\rho (d^\dagger \tilde{d})^2. \quad (3)$$

The Majorana interaction is

$$\hat{M}_{\pi\nu} = \xi_2 [(d_\nu^\dagger s_\pi^\dagger - d_\pi^\dagger s_\nu^\dagger) \cdot (\tilde{d}_\nu s_\pi - \tilde{d}_\pi s_\nu)]^{(2)} + \frac{1}{2} \sum_{k=1,3} \xi_k [d_\nu^\dagger d_\pi^\dagger]^{(k)} \cdot [\tilde{d}_\pi \tilde{d}_\nu]^{(k)}, \quad (4)$$

and it only affects the positions of the mixed symmetry states. The  $V_{\rho\rho}$  term represents the interaction between like bosons,

$$\hat{V}_{\rho\rho} = 1/2 \sum_{L=0,2,4} [2L+1] C_\rho^{(L)} [d_\rho^\dagger d_\rho^\dagger]^{(L)} \cdot [\tilde{d}_\rho \tilde{d}_\rho]^{(L)}, \quad (5)$$

where  $\rho = \pi, \nu$ .

The term  $H_F$  is the Hamiltonian of odd fermion,

$$H_F = \sum_i \epsilon_i n_i, \quad (6)$$

where  $\epsilon_i$  is the quasi-particle energy of the  $i$ th orbital, and  $n_i$  is fermion number operator. The quasi-particle energies and occupation probabilities are usually calculated using the **BCS** [36] approximation in terms of the Fermi energy  $\lambda$ , the pairing gap  $\Delta$  and the single-particle energies  $E_i$ ,

$$\epsilon_i = \sqrt{(E_i - \lambda)^2 + \Delta^2}. \quad (7)$$

The occupation probabilities are then given by

$$v_i = \left[ \frac{1}{2} \left( 1 - \frac{E_i - \lambda}{\epsilon_i} \right) \right]^{1/2}, \quad u_i = (1 - v_i^2)^{1/2}. \quad (8)$$

The bosons-fermion interaction  $V_{BF}$  is, in general, rather complicated but it has been shown [34] to be dominated by three terms,

$$V_{BF} = \sum_i A_i n_i n_{d_\rho} + \sum_{i,j} \Gamma_{ij} ([a_i^\dagger \tilde{a}_j]^{(2)}) \cdot Q_\rho^B + \sum_{i,j} \Lambda_{ki}^j \{ : [[d_\rho^\dagger \tilde{a}_j]^{(k)} a_i^\dagger s_\rho]^{(2)} : \cdot [s_\rho^\dagger \tilde{d}_\rho]^{(2)} + H.c. \}, \quad (9)$$

where  $\tilde{d}_\mu = (-1)^\mu d_{-\mu}$ ,  $\tilde{a}_{j\mu} = (-1)^{j-\mu} a_{j-\mu}$  and  $Q_\rho^B$  is the boson quadrupole operator which is defined in eq. (3). The symbols  $\rho$  and  $\rho'$  denote  $\pi(\nu)$  and  $\nu(\pi)$  if the odd fermion is a proton (neutron). The first term in Eq.(9) is a monopole-monopole interaction, which is proportional to the number of d-bosons. Therefore it only gives rise to a renormalization of the boson energy  $\varepsilon = \varepsilon_d - \varepsilon_s$  and it does not affect the main structure of energy spectrum. The second term is a quadrupole-quadrupole interaction, and the last term is the exchange interaction. The origin of the exchange force is closely related to the presence of the Pauli principle. Both terms are dominant terms and appear to arise from the strong neutron-proton quadrupole force. The orbital dependence of the coupling coefficients has been microscopically estimated [37]

$$\Gamma_{i,j} = (u_i u_j - v_i v_j) Q_{i,j}, \quad (10)$$

$$\Lambda_{k,i}^j = -\beta_{k,i} \beta_{j,k} \left( \frac{10}{N_\rho (2j_k + 1)} \right)^{1/2} \Lambda, \quad (11)$$

$$\beta_{i,j} = (u_i u_j + v_i v_j) Q_{i,j}, \quad (12)$$

$$Q_{i,j} = \langle l_i, \frac{1}{2}, j_i || Y^{(2)} || l_j, \frac{1}{2}, j_j \rangle. \quad (13)$$

### III. EVEN-EVEN NUCLEI STRUCTURE

In the calculation the proton and neutron shells are assumed to be closed at  $Z=50$  and  $N=82$  magic shells. For  $^{150,152}\text{Dy}$  nuclei, there are eight proton-bosons and one and two neutron-bosons, respectively. On the other hand, there are seven hole-like proton bosons and one and two particle-like neutron bosons for  $^{152,154}\text{Er}$  nuclei, respectively. The calculated excitation energies are obtained by diagonalizing the Hamiltonian in Eq. (2), usually using the NPBOS code [38]. The parameters  $\varepsilon_d$  and  $\kappa_{\pi\nu}$  have been determined so as to reproduce as closely as possible the energy of the low lying positive parity states. The energy of the ground state band levels were optimized by varying the proton anharmonicity parameters  $C_\pi^L$  ( $L = 0, 2, 4$ ). The parameters  $\chi_\pi$  and  $\chi_\nu$  have been kept constant in the two isotopes, and are taken as the same as those for the  $SU(3)$  limit:  $\chi_\pi = \chi_\nu = -\sqrt{7}/2$ . In order to identify mixed symmetry states, we fitted the energy of all the  $J = 2^+$  states below 3 MeV by smoothly changing  $\xi_2$ . The best fit values for the Hamiltonian parameters are given in Table I and the calculated energy levels are compared with available experimental data as shown in Figs. 1-4. Good agreement between the calculated and observed spectrum is obtained for the ground state band. From Fig. 1 one can see that the sequence of levels is well reproduced, though the calculated excitation energies of  $6_1^+$  and  $8_1^+$  are somewhat higher than the experimental ones. The splitting of  $2_2^+$  and  $4_1^+$  in the "two phonon states" is well reproduced, and it justifies the value of  $C_\pi^L$  that are used. The energy of  $0_2^+$  "of the two phonon states" equals to 1.757 MeV in the IBM-2, and this remains to be seen in future experiment.

In  $^{152}\text{Dy}$  nucleus, the level at 1.452 MeV have possible  $J = 1^+, 2^+$  assignments in experiment. It is close to a level at 1.452 MeV with  $J = 1^+$  in our IBM-2 result. The  $4_2^+$  state is higher than the data. There is no suitable solution in the present scheme for this problem. One possible explanation is the effect of the g-boson. The second  $J = 2^+$  state at energy 1.379 MeV is close to the experimental level at 1.313 MeV. The calculated  $J = 2_3^+$  state at 1.470 MeV is in good agreement with the experimental level at 1.448 MeV, and this state has mainly the  $F = F_{max}$  component. For  $^{152,154}\text{Er}$  nuclei, the ground state band fits well with data, although we used the same parameters that adjusted for  $^{150,152}\text{Dy}$  nuclei as shown in Figs. 3 and 4. In  $^{152}\text{Er}$ , the calculated  $J = 2_2^+$  state at 1.758 MeV is close to the experimental one at 1.715 MeV, and this state has a very pure  $F_{max}$  character. The calculation result shows that the wave function for  $J = 2_2^+$  is composed of 100% of the  $s^{N-2}d^2$  configuration.

### IV. ODD-PROTON $^{151,153}\text{HO}$ STRUCTURE

In order to study especially the influence of fermion degrees of freedom, we have investigated odd-neutron Dy nuclei and odd-proton Ho nuclei with the same boson parameters for each odd-A number. Thus, the differences in the nuclear structures of these two nuclei can arise only from the boson-fermion interaction and the odd-particle Hamiltonian. The quasi-particle energies  $\epsilon_i$  and occupation probabilities  $\nu^2$  are determined from a simple **BCS** calculation using Reehal and Sorensen [39] single-particle energies. The single-particle energies taken are given in Table II. The **BCS** equations are resolved with the single-particle orbitals  $g_{9/2}$ ,  $g_{7/2}$ ,  $d_{5/2}$ ,  $h_{11/2}$ ,  $d_{3/2}$  and  $s_{1/2}$ , and with  $\Delta = 12/\sqrt{A}$ . In the description of negative-parity states in Ho-isotopes, the odd proton is taken to be in the  $h_{11/2}$  orbital. We searched the optimal values of the interaction parameters that describe well the experimental levels and electromagnetic transitions. The found values of the parameters are shown in Table II. In Ho-isotopes which have 67 protons, the occupation probabilities of  $\pi h_{11/2}$  is  $\nu^2 \simeq 0.32$ . As a result, the parameter of exchange force in  $V_{BF}$  plays a crucial role in fitting the experimental data. The strength of the exchange force in the  $V_{BF}$  has to be increased in order to lower the energy of the first  $\frac{9}{2}^-$  state in  $^{153}\text{Ho}$ . The  $\Gamma$  was kept constant for both isotopes. The calculated and observed [40] energy spectra of  $^{151,153}\text{Ho}$  are shown in Figs. 5 and 6 respectively. The calculation gives a number of predictions, and they are presented in the figures which are helpful to future experiments. From the figures, we see that the calculated energy levels agree with the experimental data quite well in general. Reproduction of the trend in the experimental data is clear, especially those of the first and second appearance of negative-parity states.

Experimentally, the first and second negative parity excited states have possible  $J = (\frac{9}{2}^-, \frac{7}{2}^-)$  assignments, and they are close to states with  $J = \frac{9}{2}^-$  and  $\frac{7}{2}^-$ , respectively in the IBFM-2 calculation for both isotopes. In  $^{151}\text{Ho}$  the states at 0.869 and 0.910 MeV in the experimental data are close to the states with  $J = (\frac{13}{2}^-)_1$  and  $J = (\frac{11}{2}^-)_2$  in the IBFM-2 results at 0.826 and 0.878 MeV, respectively. The observed order inversion in Ho-isotopes, namely  $\frac{21}{2}^- - \frac{23}{2}^-$  has also been reproduced. However, the calculated energy of the  $(\frac{21}{2}^-)_1$  and  $(\frac{23}{2}^-)_1$  state in  $^{151}\text{Ho}$  are larger than the experimental value. This is probably due to the restriction of the limited single-particle space in the  $h_{11/2}$  orbital [19].

In  $^{153}\text{Ho}$  the calculated  $(\frac{15}{2}^-)_1$  state at 0.534 MeV is close to the experimental level at 0.576 MeV, while the IBFM-2 calculation gives the  $(\frac{15}{2}^-)_2$  at 1.046 MeV and it is far from the experimental one at 0.727 MeV. On other hand, the

energy of the  $(\frac{13}{2}^-)_1$  state in the model calculations equals to 0.725 MeV. We have considered two possible theoretical assignments for the experimental state at 0.926 MeV:  $\frac{5}{2}^-$  and  $\frac{9}{2}^-$ . The calculations indicate that the  $(\frac{9}{2}^-)_1$  is more probable. The characteristics of the experimental level at 1.700 MeV with possible  $(\frac{5}{2}^-, \frac{7}{2}^-, \frac{9}{2}^-)$  assignment is in good agreement with our calculated  $\frac{7}{2}^-$  state at 1.624 MeV.

The higher spin states, such as  $\frac{25}{2}^-$  and  $\frac{27}{2}^-$  of  $^{153}\text{Ho}$ , have also been reproduced. The calculated energies for the  $\frac{25}{2}^-$  and  $\frac{27}{2}^-$  states in  $^{153}\text{Ho}$  are 2.490 and 2.201 MeV, respectively, which are close to experimental levels at 2.358 and 2.297 MeV respectively.

## V. ODD-NEUTRON $^{151,153}\text{Dy}$ STRUCTURE

For Dy-isotopes, the **BCS** equations are solved with the single-particle orbitals  $f_{7/2}$ ,  $h_{9/2}$ ,  $p_{3/2}$ ,  $f_{5/2}$ ,  $i_{13/2}$ ,  $h_{11/2}$  and  $p_{1/2}$  with  $\Delta = 12/\sqrt{A}$ . The values of single-particle energies are extracted from Ref. [41], and they are very similar to the ones used in Ref. [42], except for the  $i_{13/2}$  orbital. In our calculations the  $i_{13/2}$  is still present between the  $h_{9/2}$  and  $p_{3/2}$  orbitals but close to  $p_{3/2}$  orbital in both isotopes. The adopted single-particle energies are listed in Table III. In  $^{151,153}\text{Dy}$ -isotopes, the  $\nu p_{1/2}$  level is almost completely empty ( $\nu^2 \approx 0$ ) while the  $\nu h_{11/2}$  level is almost completely occupied ( $\nu^2 \approx 1$ ), thus the two orbitals were omitted from the calculation. According to this result, we include only the first four orbitals in calculating the negative-parity states.

A comparison of the results of our IBFM-2 calculations with the experimental results [40] on the low-lying negative-parity states of  $^{151,153}\text{Dy}$  isotopes is shown in Figs. 7 and 8, respectively. All levels below 2.5 MeV known from experiment are included. From Fig. 7, one can see that the  $(\frac{9}{2}^-)_1$  and  $(\frac{11}{2}^-)_1$  states agree very well between calculation and experiment. For  $^{151}\text{Dy}$  the experimental data up to 2.5 MeV is scarce. The low-lying state with 0.984 MeV has not been assigned any other quantum number. It has a transition  $E_\gamma = 0.209$  and  $\log ft = 5.8$  from  $^{151}\text{Ho}$  ground state  $\frac{11}{2}^-$ . From our calculation, it is close to the calculated state at 0.886 MeV with  $J^- = (\frac{9}{2}^-)_2$ . This assignment is further enforced by our  $\log ft$  studies to be presented shortly.

Another state with uncertain spin assignment  $(\frac{9}{2}, \frac{11}{2}^-)$  is at an excitation energy of 1.549 MeV with  $\gamma$ -transition to  $(\frac{7}{2}^-)_1$  state, and it has a  $\log ft = 5.1$  from  $^{151}\text{Ho}$  ground state  $\frac{11}{2}^-$ . It is reproduced very well in our IBFM-2 calculation with an excitation energy of 1.523 MeV with  $J^- = (\frac{9}{2}^-)_3$ . There is not  $J^- = \frac{11}{2}^-$  state in energy range between 1.40 MeV and 1.68 MeV in our calculation. Our calculation predicts  $(\frac{3}{2}^-)_1$  and  $(\frac{3}{2}^-)_2$  at 0.657 MeV and 1.369 MeV in  $^{151}\text{Dy}$ , and they have not been observed experimentally, while in  $^{153}\text{Dy}$  the  $(\frac{3}{2}^-)_1$  state is at 0.104 MeV in our IBFM-2 calculation, and this very well reproduced the experimental level at 0.108 MeV.

In Fig. 8 we present a more detailed comparison between experimental and calculated energy states in  $^{153}\text{Dy}$ . Because many states have no clear assignment, so special attention is given to these levels with the hope to give assignment to them. Indeed, it is found that many calculated states are quite close to the experimental ones, and it will be highly desirable to substantiate this model prediction in future experiment. A detailed presentation is given in Table IV where we list the calculated energy levels, available experimental assignments (certain and uncertain spin assignment).

We also analyzed the single particle occupation probability for interested states in Dy-isotopes, and they are summarized in Table V. It is apparent that for the first few states, they are mainly single quasi-particle excited states where one of the occupation probability is dominant. As we go to higher excited states, we see a spreading of the occupation into more single particle states. The most important single-particle orbitals are those closest to the Fermi level, and they are  $f_{7/2}$  and  $h_{9/2}$ . Clearly, for  $^{153}\text{Dy}$ , the  $\frac{21}{2}^-$  state is lower than that of the  $\frac{23}{2}^-$  in energy, and there is no order inversion here.

## VI. ELECTROMAGNETIC TRANSITIONS

In the IBFM-2 model the electromagnetic transition operator is described by the following operator

$$T^{(\lambda)} = T_B^{(\lambda)} + T_F^{(\lambda)}, \quad (14)$$

which contains a boson part and fermion part. The  $E2$  transition operator is expressed [34]

$$T^{E2} = e_\pi^B Q_\pi^B + e_\nu^B Q_\nu^B + \sum_{i,j} e_{i,j}^{(2)} [a_i^\dagger \tilde{a}_j]^{(2)}, \quad (15)$$

where the quadrupole operators  $Q_\pi$  and  $Q_\nu$  are defined in Eq.(3),  $e_\pi$  and  $e_\nu$  the proton and neutron boson effective charges and

$$e_{i,j}^{(2)} = -\frac{1}{\sqrt{5}}(u_i u_j - v_i v_j) \langle l_i, \frac{1}{2}, j_i || r^2 Y^{(2)} || l_j, \frac{1}{2}, j_j \rangle. \quad (16)$$

The  $M1$  transition operator in IBFM-2 is

$$T^{M1} = \sqrt{\frac{3}{4\pi}} (g_\pi^B L_\pi^B + g_\nu^B L_\nu^B + \sum_{i,j} e_{i,j}^{(1)} [a_i^\dagger \tilde{a}_j]^{(1)}), \quad (17)$$

where  $g_\pi$  and  $g_\nu$  are  $g$  factors for proton and neutron boson,  $\tilde{L}$  is the angular momentum operator

$$L_\rho = \sqrt{10} [d_\rho^\dagger \tilde{d}_\rho]^{(1)}, \quad (18)$$

and the coefficient

$$e_{i,j}^{(1)} = -\frac{1}{\sqrt{3}}(u_i u_j + v_i v_j) \langle l_i, \frac{1}{2}, j_i || (g_l \mathbf{l} + g_s \mathbf{s}) || l_j, \frac{1}{2}, j_j \rangle, \quad (19)$$

where  $g_l$  and  $g_s$  are the single particle  $g$ -factors of the odd nucleon. For boson part, the  $E2$  matrix elements are very sensitive to the difference between neutron boson and proton effective charge, and they are kept constant at  $e_\pi = 2e_\nu = 0.1 e.b$  for all isotopes. The values of  $e_\rho^B$  were determined from the experimental  $B(E2; 2_1^+ \rightarrow 0_1^+)$  of even-even  $^{152}\text{Dy}$  nucleus. For the odd nucleon, the effective charge  $1.5 e$  and  $0.5 e$  are taken for the proton and the neutron, respectively. The parameter  $\chi$  in the  $E2$  transition operator has the same value as in the Hamiltonian, though they are not necessary [43, 44]. The standard boson  $g$  factor values  $g_\pi = 1 \mu_N$  and  $g_\nu = 0 \mu_N$  are used for all isotopes. We have estimated the single particle  $g_l$  and  $g_s$ , and taken them as  $g_{l,\nu}^F = 0 \mu_N$  and  $g_{l,\pi}^F = 1 \mu_N$ , while the spin  $g$ -factors are taken as the free values quenched by a factor of 0.7 and 0.5 for proton and neutron, respectively, which is the common practice as in Refs. [20, 45, 46]. Using this procedure we have calculated the electromagnetic transitions, and a very good agreement between calculated and experimental magnetic moment of the ground states is obtained in both magnitude and sign as shown in Tables X and XI.

The resulting branching ratios for the  $^{151,153}\text{Ho}$  and  $^{151,153}\text{Dy}$  nuclei are listed in Tables VI-IX, respectively, in comparison with the experimental data [40]. In these tables, the strongest branch is correctly predicted. The other transitions are in qualitative agreement with experiment. The deviations can be reduced by changing  $g_s$ , as well as by changing the effective charges. From Tables V, VIII and IX, one can see that the strongest transitions are between those states having the same dominated single-particle orbital. This means that a strong transition should occur between levels in the same band. Our results for electromagnetic transition probabilities are summarized in Tables X and XI respectively. In  $^{151,153}\text{Dy}$  the  $\frac{5}{2}_1^-$  states decay predominantly to the  $\frac{3}{2}_1^-$  states via a pure  $M1$  transition. In  $^{153}\text{Dy}$  isotope, the  $\frac{5}{2}_1^-$  is associated with  $\nu f_{7/2}$  and  $\nu h_{9/2}$ , the exhibit sizable mixing of these two quasi-particle orbitals. Due to the mixing of the two components in the wave function in this state, the  $\frac{5}{2}_1^-$  and  $\frac{7}{2}_1^-$  states are connected by strong  $E2$  transition and weak  $M1$  transition in  $^{153}\text{Dy}$  isotope. In contrast, we see that the  $\frac{5}{2}_1^-$  state decays to  $\frac{7}{2}_1^-$  states by very strong  $E2$  and  $M1$  transitions in  $^{151}\text{Dy}$  isotope.

We have also calculated the quadrupole moments of the ground states and some low-lying states in  $^{151,153}\text{Ho}$  and  $^{151,153}\text{Dy}$ . The results are given in Tables X and XI respectively. The calculated results are in the same order of magnitude as the available experimental data.

## VII. $\beta$ -DECAY

In IBFM-2, a relation among the IBM and the underlying shell model has been established by including the proton and neutron degree of freedom [7]. This offers one the capability to compute the probabilities of  $\beta$ -decay. The decay of odd-nuclei proceeds predominantly through the conversion of the odd particle from neutron to proton ( $\beta^-$ -decay) or from proton to neutron ( $\beta^+$ -decay). There are two types of beta decay, the Fermi decay and Gamow-Teller decay. In the framework of IBFM both transitions can be calculated [47]. First define the following operators,

$$A_m^{\dagger(j)} = \zeta_j a_{jm}^\dagger + \sum_{\dot{j}} \zeta_{j\dot{j}} s^\dagger [\tilde{d} a_{\dot{j}m}^\dagger]^{(j)} \quad (\Delta n_j = 1, \Delta N = 0), \quad (20)$$

$$B_m^{\dagger(j)} = \Theta_j s^\dagger \tilde{a}_{jm} + \sum_j \Theta_{jj} [d^\dagger \tilde{a}_j]_m^{(j)} \quad (\Delta n_j = -1, \Delta N = 1), \quad (21)$$

$$\tilde{A}_m^{(j)} = (-1)^{j-m} \{A_{-m}^{\dagger(j)}\}^\dagger = \zeta_j^* \tilde{a}_{jm} + \sum_j \zeta_{jj}^* s [d^\dagger \tilde{a}_j]_m^{(j)} \quad (\Delta n_j = -1, \Delta N = 0), \quad (22)$$

$$\tilde{B}_m^{(j)} = (-1)^{j-m} \{B_{-m}^{\dagger(j)}\}^\dagger = -\Theta_j^* s a_{jm}^\dagger - \sum_j \Theta_{jj}^* [\tilde{d} a_j^\dagger]_m^{(j)} \quad (\Delta n_j = 1, \Delta N = -1). \quad (23)$$

Then the Fermi and the Gamow-Teller transition operators are

$$Q^F = \sum_j -\sqrt{2j+1} [P_\pi^{(j)} P_\nu^{(j)}]^{(0)}, \quad (24)$$

$$Q^{GT} = \sum_{jj} \eta_{jj} [P_\pi^{(j)} P_\nu^{(j)}]^{(1)}, \quad (25)$$

where

$$\eta_{jj} = -\frac{1}{\sqrt{3}} \langle l, \frac{1}{2}, j \| \sigma \| l, \frac{1}{2}, j \rangle = -\delta_{ll} \sqrt{2(2j+1)(2j+1)} W(lj \frac{1}{2} 1; \frac{1}{2} j). \quad (26)$$

The form of transfer operator  $P_\rho^j$  depends on the specific nuclei, and in the present case,  $P_\pi^{(j)} = \tilde{A}_\pi^{(j)}$  and  $P_\nu^{(j)} = \tilde{B}_\nu^{(j)}$ . The  $ft$  value is calculated by

$$ft = \frac{6163}{\langle M_F \rangle^2 + (G_A/G_V)^2 \langle M_{GT} \rangle^2} \quad (27)$$

in units of second where  $G_A/G_V^2=1.59$ , and

$$\langle M_F \rangle^2 = \frac{1}{2I_i + 1} |\langle I_f \| Q^F \| I_i \rangle|^2, \quad (28)$$

$$\langle M_{GT} \rangle^2 = \frac{1}{2I_i + 1} |\langle I_f \| Q^{GT} \| I_i \rangle|^2. \quad (29)$$

Having obtained the wave functions, we can calculate the  $\beta$ -decay rates. It should be stressed that there is no adjustable parameters in the beta decay calculation, consequently the  $\log_{10} ft$  is obtained in a parameter free manner. Examining the wave function of daughter nuclei  $^{151,153}\text{Dy}$ , the first and second excited  $\frac{9}{2}^-$  states are dominated by  $h_{9/2}$  and  $f_{7/2}$  orbitals in both isotopes, respectively. According to these components the  $\log_{10} ft$  values of the two states have the approximately the same values and in good agreement with experimental ones. An interesting result of the calculation is that it indicates the observed state at 1.549 MeV in  $^{151}\text{Dy}$ , corresponds to the state  $(\frac{9}{2}^-)_3$  at 1.523 MeV in the IBFM-2 result, and the main single-particle component of this state is  $h_{9/2}$ . Because the  $(\frac{9}{2}^-)_3$  state in  $^{153}\text{Dy}$  at 0.862 MeV in IBFM-2 results, has a dominant component of  $f_{7/2}$ , the beta decay rate is small, hence the  $\log_{10} ft$  value of the  $(\frac{9}{2}^-)_3$  in  $^{153}\text{Dy}$  is larger than for the one in  $^{151}\text{Dy}$ . This enforces our spin assignment in the structure calculation.

The  $\beta$ -decays of ground state  $J^- = \frac{11}{2}^-$  of  $^{151,153}\text{Ho}$  to  $^{151,153}\text{Dy}$  have many branches as shown in Table XII, but the strong ones are to the level  $\frac{9}{2}_1^-$ , which are 60 and 70 percent [48]. The  $\log_{10} ft$  are equal to ( 4.6 and 3.511) and (4.7 and 3.612) in the experiments and the model results for two isotopes, respectively. In  $^{153}\text{Dy}$ , with the predicted assignments  $J^-(1.092)$  and  $J^-(1.189) = \frac{11}{2}^-$ , the calculated  $\log_{10} ft$  of the two branches are 6.707 and 7.358 respectively, which are close to the experimental value of 6.3 for both branches, respectively.

From Table XII, it can be concluded that IBFM-2 provides a meaningful framework for describing  $\beta$ -decay transitions between  $^{151,153}\text{Dy}$  and  $^{151,153}\text{Ho}$ . Together with other recent  $\beta$ -decay calculations [33, 34, 35], it shows that the IBFM-2 is well suited for understanding  $\beta$ -decay properties of rare-earth nuclei.

## VIII. SUMMARY

In this work IBFM-2 calculations for the odd-mass Ho and Dy (A=151,153) have been presented. For Dy-isotopes four fermion single-particle  $f_{7/2}$ ,  $h_{9/2}$ ,  $p_{3/2}$  and  $f_{5/2}$  orbitals were used to study the negative- parity states. For

study the negative- parity states in Ho-isotopes only  $h_{11/2}$  has been taken into account. The boson-boson interaction parameters were fixed by the calculation on the boson core nuclei. The boson-fermion interaction parameter is kept constant of each element, and there are only two free varying boson-fermion quadrupole interaction parameters for each even-odd nucleus. The analysis of the wave functions indicates that the  $f_{7/2}$  and  $h_{9/2}$  orbitals are dominate in the wave functions in Dy-isotopes. The known quadrupole and magnetic moments in these nuclei are reasonably well described by the model. The present IBFM-2 calculations provide a satisfactory framework for describing the  $\beta$ -decay rates in the odd-mass nuclei with  $A \sim 150$ . The predictions of this work can serve as a good reference to experimentalists. Further experimental study will be very helpful to further test the present IBFM-2 calculation.

### Acknowledgements

The authors would like express their thanks to Professor N. Yoshida for his interest in the subject and his many helpful suggestions. This work is supported by the National Fundamental Research Program Grant No. 2006CB921106, China National Natural Science Foundation Grant Nos. 10325521, 60433050 and the SRFDP program of Education Ministry of China.

- 
- [1] P. Van Isacker and G. Puddu, Nucl. Phys. **A 348**, 125 (1980).
  - [2] A. Sevrin, K. Heyde and J. Jolie, Phys Rev. **C 36**, 2621 (1987).
  - [3] K. Kim, A. Gelberg, T. Mizusaki, T. Otsuka and P. Von Brentano, Nucl.Phys. **A 604**, 163 (1996).
  - [4] A. Arima and F. Iachello, Ann. Phys. **99**, 253 (1976 ).
  - [5] A. Arima and F. Iachello, Ann. Phys. **111**, 201 (1978).
  - [6] A. Arima and F. Iachello, Ann. Phys. **123**, 468 (1979).
  - [7] F. Iachello and A. Arima, *The Interacting Boson Model* (Cambridge University Press, NewYork, 1987).
  - [8] W. D. Hamilton, A. Irbäck and J. P. Elliott, Phys. Rev. Lett. **53**, 2469 (1984).
  - [9] P.E. Garrett, H. Lehmann, C.A. McGrath, Minfang Yeh and S.W. Yates, Phys. Rev. **C 54**, 2259 (1996).
  - [10] A. Gade, H. Klein, N. Pietralla and P. von Brentano, Phys. Rev. **C 65**, 054311 (2002).
  - [11] E. Elhami, J.N. Orce, S. Mukhopadhyay, S.N. Choudry, M. Scheck, M.T. McEllistrem, and S.W. Yates, Phys. Rev. **C 75**, 011301(R) (2007).
  - [12] J.P. Elliott, P.A. White, Phys. Lett. **B 97**, 169 (1980).
  - [13] J.P. Elliott, J.A. Evans and V.S. Lac, Nucl. Phys. **A 597**, 341 (1996).
  - [14] J.A. Evans, J.P. Elliott, V.S. Lac and G. L. Long, Nucl. Phys. **A 593**, 85 (1995).
  - [15] E.J. Garcia-Ramos and P. Van Isacker, Ann. Phys. **274**, 45 (1999).
  - [16] F.H. Al-Khudair, Y.S. Li and G.L. Long, J. Phys. Nucl. Part Phys. **G 30**, 1287 (2004).
  - [17] F.H. Al-Khudair, Y.S. Li and G.L. Long, Phys. Rev. **C 75**, 054316 (2007).
  - [18] F. Iachello and O. Scholten, Phys Rev. Lett. **43**, 679 (1979).
  - [19] M.A. Cunningham, Nucl. Phys. **A 385**, 204 (1982); **A 385**, 221 (1982).
  - [20] J.M. Arias, C.E. Alonso and R. Bijker, Nucl. Phys. **A 445**, 333 (1985) .
  - [21] G. Lhersonneau, B. Pfeiffer, K.L. Kratz, H. Ohm, K. Sistemich, S. Brant and V. Paar, Z. Phys. A-Atomic Nuclei **337**, 149 (1990).
  - [22] N. Yoshida, A. Gelberg, T. Otsuka, I. Wiedenhöver, H. Sagawa and P. Von Brentano, Nucl. Phys. **A 619**, 65 (1997).
  - [23] S. Brant, V. Paar and A. Wolf, Phys. Rev. **C 58**, 1349 (1998).
  - [24] H. R. Yazar and I. Uluer, Phys. Rev. **C 75**, 034309 (2007).
  - [25] P. Sarriguren, E. Moya de Guerra, and A. Escuderos, Phys. Rev. **C 64**, 064306 (2001).
  - [26] S. Harissopulos, J. Döring, M. La Commara, K. Schmidt, C. Mazzocchi, R. Borcea, S. Galanopoulos, M. Górska, H. Grawe, M. Hellström, Z. Janas, R. Kirchner, E. Roeckl, I.P. Johnstone, R. Schwengner, and L. D. Skouras, Phys. Rev. **C 72**, 024303 (2005).
  - [27] I.S. Towner and J.C. Hardy, Phys. Rev. **C 66**, 035501 (2002).
  - [28] I.N. Borzov, Phys. Rev. **C 67**, 025802 (2003).
  - [29] K. Chaturvedi, B.M. Dixit, P.K. Rath, and P.K. Raina, Phys. Rev. **C 67**, 064317 (2003).
  - [30] G. Lhersonneau and S. Brant, Phys. Rev. **C 72**, 034308 (2005).
  - [31] M.T. Mustonen, M. Aunola and J. Suhonen, Phys. Rev. **C 73**, 054301 (2006).
  - [32] S. M. Fischer, C.J. Lister, N.J. Hammond, R.V.F. Janssens, T.L. Khoo, T. Lauritsen, E. F. Moore, D. Seweryniak, S. Sinha, D.P. Balamuth, P.A. Hausladen, D.G. Sarantites, W. Reviol, P. Chowdury, S.D. Paul, C. Baktash and C.H. Yu, Phys. Rev. **C 74**, 054304 (2006).
  - [33] N. Yoshida, L. Zuffi and S. Brant, Phys. Rev. **C 66**, 014306 (2002).
  - [34] L. Zuffi, S. Brant and N. Yoshida, Phys. Rev **C 68**, 034308 (2003).
  - [35] S. Brant, N. Yoshida and L. Zuffi, Phys. Rev. **C 70**, 054301 (2004).
  - [36] J. Bardeen, N.L. Cooper and J.R. Schrieffer, Phys. Rev. **108**, 1175 (1957).

- [37] O. Schoiten and A.E.L. Dieperink, in *Interacting Boson-Fermi Systems in Nuclei*, ed. F. Iachell, (Plenum, New York, 1981).
- [38] T. Otsuka, N. Yoshida, Program NPBOS , Japan Atomic Energy Research Insitute report JAERI-M85-094 (1985).
- [39] B. S. Reehal and R. Sorensen, *Phys. Rev. C* **2**, 819 (1970).
- [40] <http://www.nnd.bnl.gov/ensdf/>, "Evaluated Nuclear Structure Data File" (ENSDF), (2007).
- [41] A. Boher and B.R. Mottelson, *Nuclear structure*, (Benjamin,INC New York 1975).
- [42] R. Bijker and A.E.L. Dieperink, *Nucl. Phys. A* **379**, 239 (1982).
- [43] G.L. Long and H.Y. Ji, *Phys. Rev. C* **57**, 1686 (1998).
- [44] G.L. Long, *Commun. Theor. Phys.* **32**, 489 (1999).
- [45] C.E. Alonso, J.M Arias and M. Lozano, *J. Phys. Nucl. Phys.* **G 13**, 1269 (1987).
- [46] A. Gizon, J. Genevey, D. Bucurescu, Gh Căta-Danil, J. Gizon, J.Inchaouh, D. Barnéoud, T. Von Egidy C.F. Liag, B.M. Nyakó, P. Paris, I. Penev, A. Plochocki, E. Ruchowska, C.A. Ur, B. Weiss and L. Zolnai, *Nucl. Phys. A* **605**, 301 (1996).
- [47] F. Dellagiacoma, Ph.D. thesis, Yale University, (1988); F. Dellagiacoma and F. Iachello, *Phys. Lett. B* **218** 399 (1989).
- [48] R.B.Firestone, *Table of Isotopes*, edited by Virginia S. Shirley (John Wiley and Sons, New York, 1998).

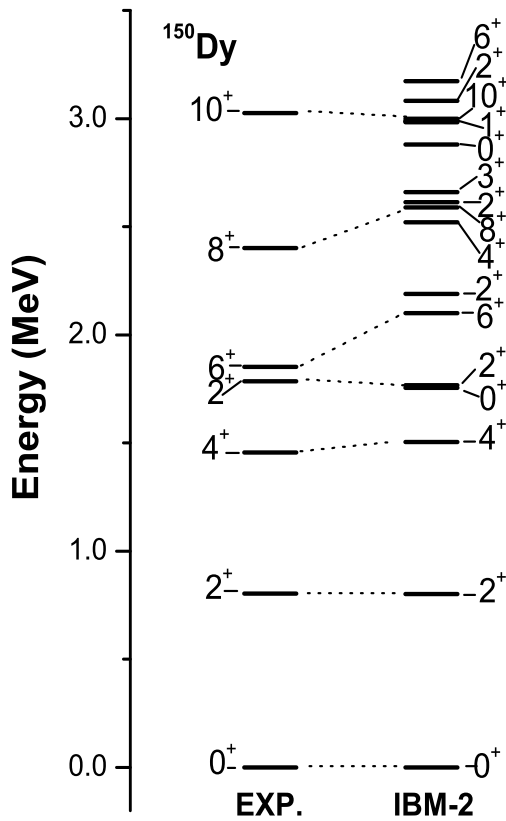


FIG. 1: The calculated and observed energy spectra for the  $^{150}\text{Dy}$  isotope.

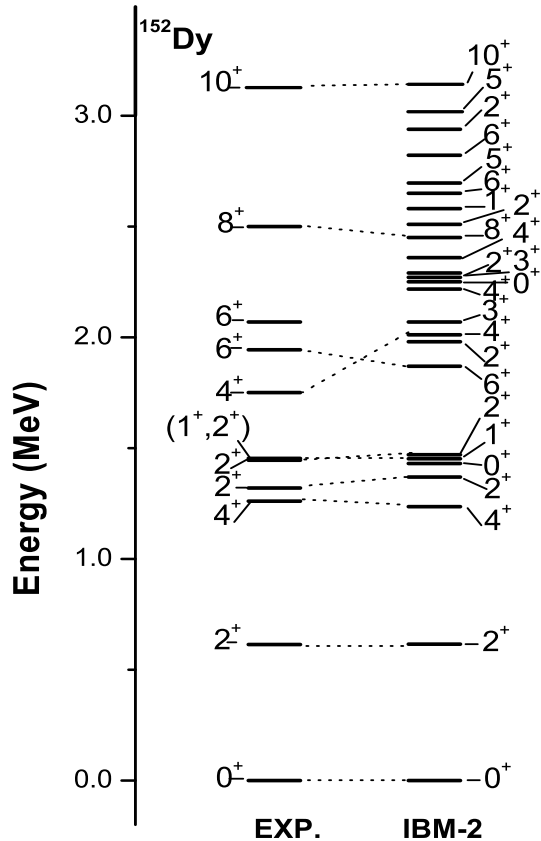


FIG. 2: The calculated and observed energy spectra for the  $^{152}\text{Dy}$  isotope.

TABLE I: The parameters of the IBM-2 Hamiltonian.  $\chi_\pi = \chi_\nu = -1.323$ , have been chosen for  $^{150,152}\text{Dy}$  and  $^{152,154}\text{Er}$ . All the parameters are in MeV unit.

nucleus	$\kappa_{\pi\nu}$	$\varepsilon_d$	$\xi_1$	$\xi_2$	$\xi_3$	$C_\pi^L(L=0,2,4)$
$^{150}\text{Dy}, ^{152}\text{Er}$	-0.010	0.820	0.300	0.300	0.300	0.210,0.210,-0.130
$^{152}\text{Dy}, ^{154}\text{Er}$	-0.010	0.650	-0.400	0.140	0.400	0.500,0.500,0.000

TABLE II: Single-particle energies (MeV) of proton orbitals in Ho-isotopes and parameters in the boson-fermion interaction (MeV).

nucleus	$g_{9/2}$	$g_{7/2}$	$d_{5/2}$	$h_{11/2}$	$d_{3/2}$	$s_{1/2}$	$\Gamma$	$A$	$\Lambda$
$^{151}\text{Ho}$	-5.000	0.123	0.800	2.202	3.021	3.277	1.200	-0.500	0.250
$^{153}\text{Ho}$	-5.000	0.148	0.798	2.252	3.101	3.337	1.200	-0.240	0.520

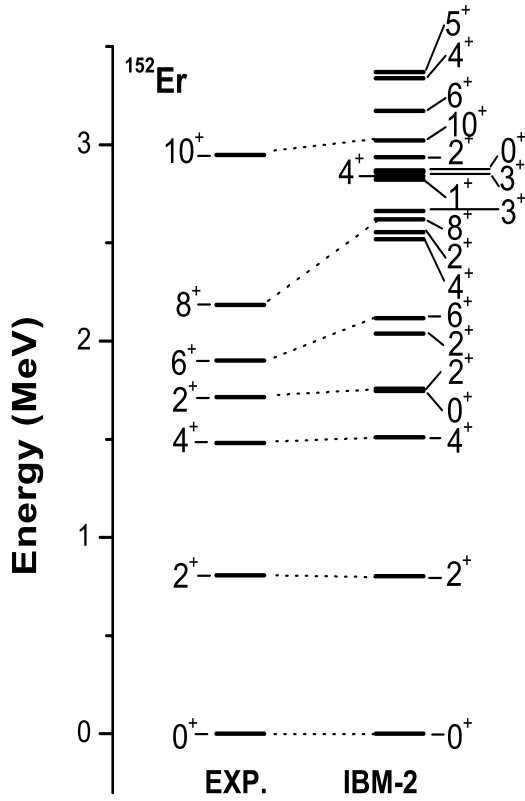


FIG. 3: The calculated and observed energy spectra for the <sup>152</sup>Er isotope.

TABLE III: Single-particle energies (MeV) of neutron orbitals in Dy-isotopes and parameters in the boson-fermion interaction (MeV).

nucleus	$h_{11/2}$	$h_{9/2}$	$f_{7/2}$	$f_{5/2}$	$i_{13/2}$	$p_{3/2}$	$p_{1/2}$	$\Gamma$	$A$	$\Lambda$
<sup>151</sup> Dy	-5.800	-0.4300	-1.450	1.760	1.350	1.450	2.740	0.500	-0.300	0.350
<sup>153</sup> Dy	-5.800	-0.450	-1.500	1.800	1.350	1.500	2.800	0.500	-0.440	0.550

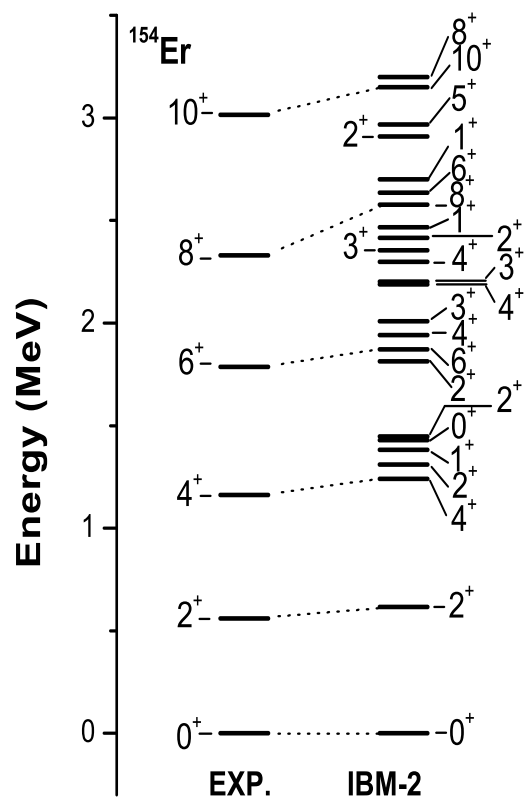


FIG. 4: The calculated and observed energy spectra for the  $^{154}\text{Er}$  isotope.

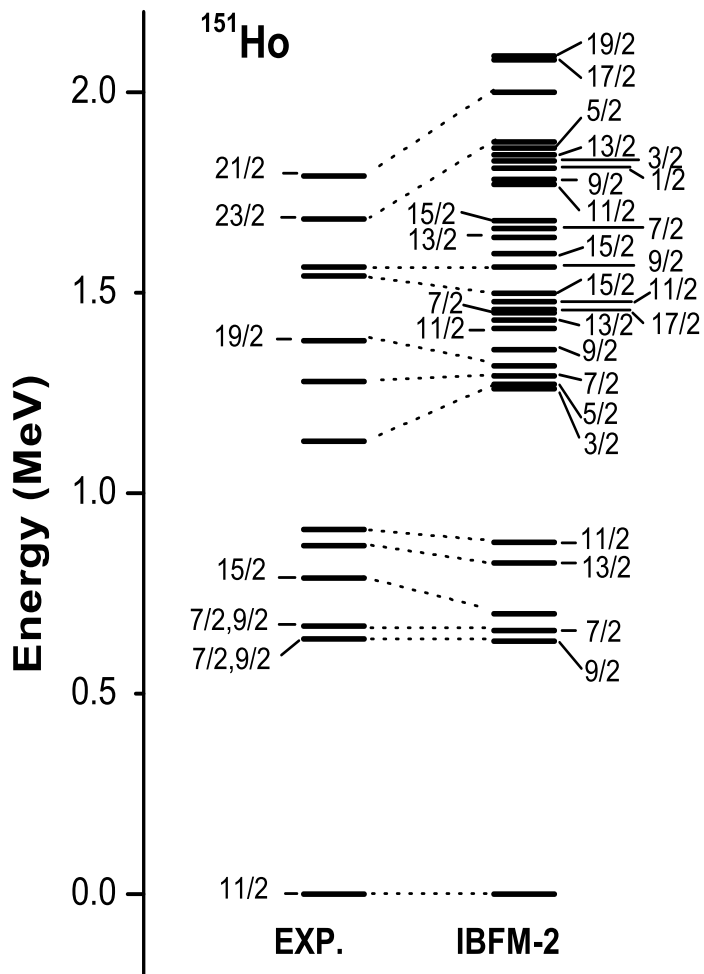


FIG. 5: The calculated and observed energy spectra for the <sup>151</sup>Ho isotope.

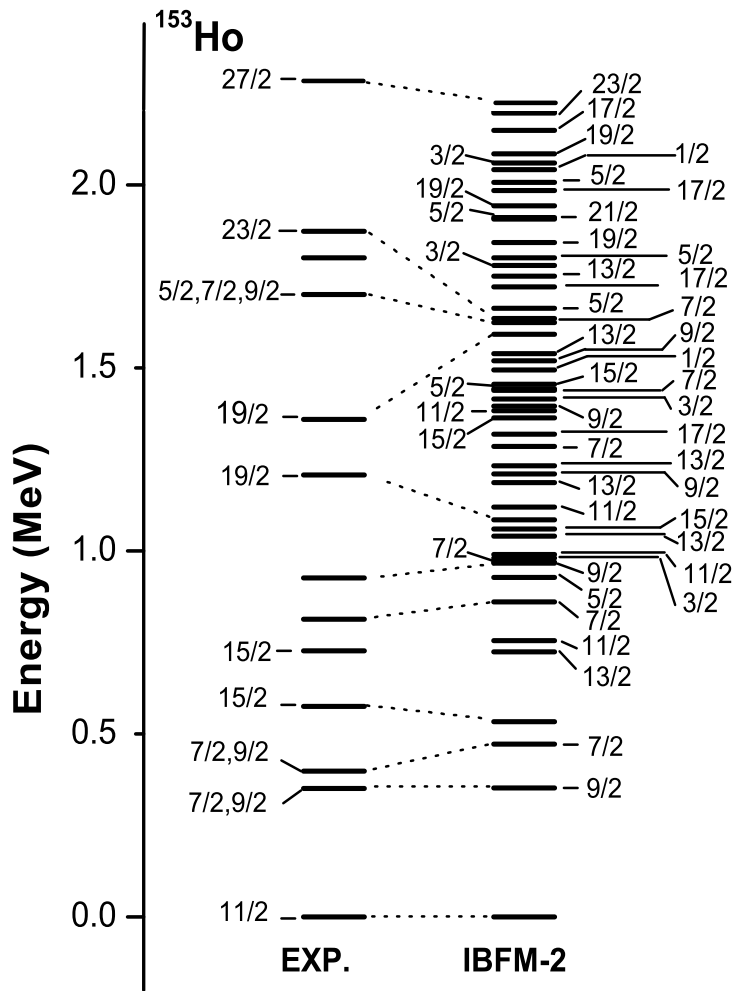


FIG. 6: The calculated and observed energy spectra for the <sup>153</sup>Ho isotope.

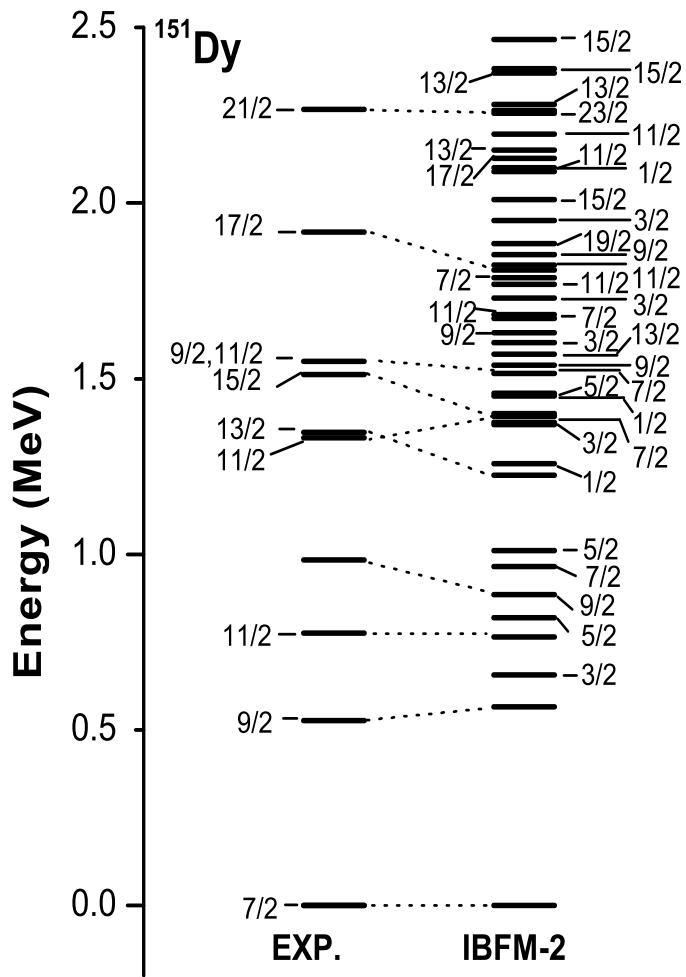


FIG. 7: The calculated and observed energy spectra for the  $^{151}\text{Dy}$  isotope.

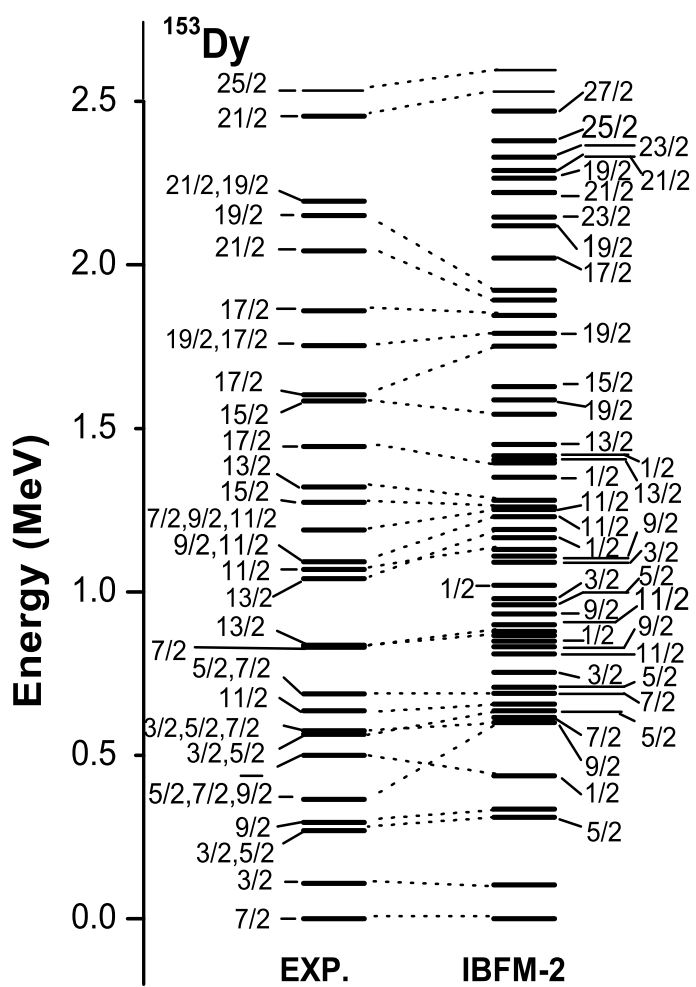


FIG. 8: The calculated and observed energy spectra for the <sup>153</sup>Dy isotope.

TABLE IV: Available experimental and calculated energy levels for  $^{153}\text{Dy}$  isotope. For details calculation see figure 8.

<u>IBFM-2</u>		<u>EXP.</u>	
$J^-$	Energy	$J^-$	Energy
$7^-/2$	0.000	$7^-/2$	0.000
$3^-/2$	0.104	$3^-/2$	0.108
$5^-/2$	0.327	$3^-/2, 5^-/2$	0.270
$9^-/2$	0.331	$9^-/2$	0.295
$1^-/2$	0.438	(-)	0.500
$9^-/2$	0.600	$5^-/2, 7^-/2, 9^-/2$	0.365
$7^-/2$	0.606	$3^-/2, 5^-/2, 7^-/2$	0.576
$5^-/2$	0.646	$3^-/2, 5^-/2$	0.565
$11^-/2$	0.657	$11^-/2$	0.637
$7^-/2$	0.695	$5^-/2, 7^-/2$	0.688
$7^-/2$	0.879	$7^-/2$	0.830
$13^-/2$	0.877	$13^-/2$	0.837
$13^-/2$	1.195	$13^-/2$	1.041
$11^-/2$	1.151	$11^-/2$	1.068
$11^-/2$	1.236	$9^-/2, 11^-/2$	1.092
$11^-/2$	1.252	$7^-/2, 9^-/2, 11^-/2$	1.189
$15^-/2$	1.254	$15^-/2$	1.273
$13^-/2$	1.277	$13^-/2$	1.321
$17^-/2$	1.394	$17^-/2$	1.455
$15^-/2$	1.543	$15^-/2$	1.584
$17^-/2$	1.752	$17^-/2$	1.602
$19^-/2$	1.796	$19^-/2, 17^-/2$	1.753
$17^-/2$	1.846	$17^-/2$	1.862
$21^-/2$	1.892	$21^-/2$	2.043
$19^-/2$	1.922	$19^-/2$	2.150
$21^-/2$	2.288	$21^-/2$	2.454
$25^-/2$	2.621	$25^-/2$	2.523

TABLE V: The percentage components of wave functions for  $^{151,153}\text{Dy}$ -isotopes.

$J^-$	$^{151}\text{Dy}$				$^{153}\text{Dy}$			
	$p_{3/2}$	$f_{7/2}$	$h_{9/2}$	$f_{5/2}$	$p_{3/2}$	$f_{7/2}$	$h_{9/2}$	$f_{5/2}$
$7/2_1^-$	2	97	0	0	2	97	1	0
$3/2_1^-$	13	86	1	1	9	90	0	1
$5/2_1^-$	2	95	1	1	2	80	17	1
$9/2_1^-$	0	6	90	4	0	1	94	4
$1/2_1^-$	18	78	2	1	15	82	2	1
$9/2_2^-$	1	91	7	0	1	93	5	0
$7/2_2^-$	4	95	1	0	8	90	1	1
$5/2_2^-$	1	4	81	14	4	53	38	5
$11/2_1^-$	5	93	1	0	3	95	1	0
$7/2_3^-$	0	5	90	4	3	46	49	2
$5/2_3^-$	13	83	4	1	8	64	22	6
$3/2_2^-$	12	85	1	1	8	88	3	1
$9/2_3^-$	1	14	81	4	4	92	4	0
$3/2_3^-$	1	10	75	14	13	77	9	2
$11/2_2^-$	0	8	89	3	5	91	3	1
$13/2_1^-$	0	6	87	7	0	1	93	6
$1/2_2^-$	1	5	78	17	10	50	34	7
$11/2_3^-$	5	88	6	1	0	3	93	3
$13/2_2^-$	3	87	9	1	0	6	89	5
$15/2_1^-$	10	88	1	1	5	94	1	0
$17/2_1^-$	1	8	82	9	0	0	92	8
$19/2_1^-$	16	81	2	1	60	39	0	1
$21/2_1^-$	3	13	74	10	0	0	91	9
$23/2_1^-$	24	73	2	1	57	41	1	1
$25/2_1^-$	15	32	45	8	1	1	88	10

TABLE VI: Branching ratios in  $^{151}\text{Ho}$  isotope, the order of states corresponding to IBFM-2 calculation.

Level (MeV)	Transition	$I_\gamma(\text{IBFM-2})$	$I_\gamma(\text{Exp.})$
0.638	$9^-/2_1 \rightarrow 11^-/2_1$	100	100
0.667	$7^-/2_1 \rightarrow 9^-/2_1$	0.1	
	$7^-/2_1 \rightarrow 11^-/2_1$	100	100
0.789	$15^-/2_1 \rightarrow 11^-/2_1$	100	100
0.869	$13^-/2_1 \rightarrow 15^-/2_1$	0.2	
	$13^-/2_1 \rightarrow 9^-/2_1$	0.0	9.7(12)
	$13^-/2_1 \rightarrow 11^-/2_1$	100	100(9)
0.910	$11^-/2_2 \rightarrow 13^-/2_1$	0.0	
	$11^-/2_2 \rightarrow 15^-/2_1$	0.0	
	$11^-/2_2 \rightarrow 7^-/2_1$	0.0	
	$11^-/2_2 \rightarrow 9^-/2_1$	7.3	
	$11^-/2_2 \rightarrow 11^-/2_1$	100	
1.129	$5^-/2_1 \rightarrow 7^-/2_1$	100	38(3)
	$7^-/2_2 \rightarrow 9^-/2_1$	43.7	
1.279	$7^-/2_2 \rightarrow 5^-/2_1$	25.4	
	$7^-/2_2 \rightarrow 11^-/2_1$	0.6	
	$7^-/2_2 \rightarrow 7^-/2_1$	69.4	
	$7^-/2_2 \rightarrow 9^-/2_1$	100	100
	$7^-/2_2 \rightarrow 11^-/2_1$	10.3	
1.387	$19^-/2_1 \rightarrow 15^-/2_1$	100	100
1.541	$7^-/2_3 \rightarrow 5^-/2_1$	0.0	
	$7^-/2_3 \rightarrow 7^-/2_2$	0.0	
	$7^-/2_3 \rightarrow 11^-/2_2$	0.5	
	$7^-/2_3 \rightarrow 7^-/2_1$	100	100
	$7^-/2_3 \rightarrow 9^-/2_1$	85.5	
	$7^-/2_3 \rightarrow 11^-/2_1$	70.6	

TABLE VII: Branching ratios in  $^{153}\text{Ho}$  isotope, the order of states corresponding to IBFM-2 calculation.

Level (MeV)	Transition	$I_\gamma(\text{IBFM-2})$	$I_\gamma(\text{Exp.})$
0.351	$9^-/2_1 \rightarrow 11^-/2_1$	100	100
0.398	$7^-/2_1 \rightarrow 9^-/2_1$	7.9	
	$7^-/2_1 \rightarrow 11^-/2_1$	100	100
0.576	$15^-/2_1 \rightarrow 11^-/2_1$	100	100
0.706	$13^-/2_1 \rightarrow 15^-/2_1$	0.7	
	$13^-/2_1 \rightarrow 9^-/2_1$	0.3	
	$13^-/2_1 \rightarrow 11^-/2_1$	100	
0.814	$7^-/2_2 \rightarrow 7^-/2_1$	0.5	
	$7^-/2_2 \rightarrow 9^-/2_1$	100	100
	$7^-/2_2 \rightarrow 11^-/2_1$	0.1	
0.926	$9^-/2_2 \rightarrow 7^-/2_2$	4.8	
	$9^-/2_2 \rightarrow 13^-/2_1$	0.0	
	$9^-/2_2 \rightarrow 7^-/2_1$	62.5	
	$9^-/2_2 \rightarrow 9^-/2_1$	54.7	100
1.207	$19^-/2_1 \rightarrow 15^-/2_1$	100	100

TABLE VIII: Branching ratios in  $^{151}\text{Dy}$  isotope, the order of states corresponding to IBFM-2 calculation.

Level (MeV)	Transition	$I_\gamma(\text{IBFM-2})$	$I_\gamma(\text{Exp.})$
0.527	$9^-/2_1 \rightarrow 7^-/2_1$	100	100
0.775	$11^-/2_1 \rightarrow 9^-/2_1$	5.1	
	$11^-/2_1 \rightarrow 7^-/2_1$	100	100
0.984	$9^-/2_2 \rightarrow 11^-/2_1$	5.0	100
	$9^-/2_2 \rightarrow 9^-/2_1$	0.1	
	$9^-/2_2 \rightarrow 7^-/2_1$	100	
1.334	$11^-/2_2 \rightarrow 9^-/2_2$	0.1	22(13)
	$11^-/2_2 \rightarrow 11^-/2_1$	0.0	50(13)
	$11^-/2_2 \rightarrow 9^-/2_1$	100	
	$11^-/2_2 \rightarrow 7^-/2_1$	0.2	
1.348	$13^-/2_1 \rightarrow 11^-/2_2$	0.0	
	$13^-/2_1 \rightarrow 9^-/2_2$	0.0	
	$13^-/2_1 \rightarrow 11^-/2_1$	0.8	7.5(15)
	$13^-/2_1 \rightarrow 9^-/2_1$	100	100(2)
1.511	$15^-/2_1 \rightarrow 13^-/2_1$	1.7	
	$15^-/2_1 \rightarrow 11^-/2_2$	0.0	
	$15^-/2_1 \rightarrow 11^-/2_1$	100	100(3)
1.549	$9^-/2_3 \rightarrow 13^-/2_1$	0.0	
	$9^-/2_3 \rightarrow 11^-/2_2$	5.6	
	$9^-/2_3 \rightarrow 9^-/2_2$	0.3	
	$9^-/2_3 \rightarrow 11^-/2_1$	23.9	
	$9^-/2_3 \rightarrow 9^-/2_1$	100	36(8)
	$9^-/2_3 \rightarrow 7^-/2_1$	3.5	100(7)
1.918	$17^-/2_1 \rightarrow 15^-/2_1$	0.6	43.2(13)
	$17^-/2_1 \rightarrow 13^-/2_1$	100	100(2)
2.263	$21^-/2_1 \rightarrow 17^-/2_1$	100	100

TABLE IX: Branching ratios in  $^{153}\text{Dy}$  isotope, the order of states corresponding to IBFM-2 calculation.

Level (MeV)	Transition	$I_\gamma(\text{IBFM-2})$	$I_\gamma(\text{Exp.})$
0.108	$3^-/2_1 \rightarrow 7^-/2_1$	100	100
0.270	$5^-/2_1 \rightarrow 3^-/2_1$	100	100(5)
	$5^-/2_1 \rightarrow 7^-/2_1$	20.2	86(4)
0.295	$9^-/2_1 \rightarrow 5^-/2_1$	0.0	
	$9^-/2_1 \rightarrow 7^-/2_1$	100	100
0.365	$9^-/2_2 \rightarrow 9^-/2_1$	0.2	
	$9^-/2_2 \rightarrow 5^-/2_1$	0.0	$\approx 3.3$
	$9^-/2_2 \rightarrow 7^-/2_1$	100	100(27)
0.565	$5^-/2_2 \rightarrow 9^-/2_2$	0.0	
	$5^-/2_2 \rightarrow 9^-/2_1$	2.0	
	$5^-/2_2 \rightarrow 5^-/2_1$	11.3	
	$5^-/2_2 \rightarrow 3^-/2_1$	50.9	100(4)
	$5^-/2_2 \rightarrow 7^-/2_1$	100	48(15)
0.576	$7^-/2_2 \rightarrow 5^-/2_2$	0.0	
	$7^-/2_2 \rightarrow 9^-/2_2$	38.5	
	$7^-/2_2 \rightarrow 9^-/2_1$	1.4	
	$7^-/2_2 \rightarrow 5^-/2_1$	100	
	$7^-/2_2 \rightarrow 3^-/2_1$	30.7	88(15)
	$7^-/2_2 \rightarrow 7^-/2_1$	72.9	100(19)
0.637	$11^-/2_1 \rightarrow 7^-/2_2$	0.0	
	$11^-/2_1 \rightarrow 9^-/2_2$	71.6	
	$11^-/2_1 \rightarrow 9^-/2_1$	19.3	1.2
	$11^-/2_1 \rightarrow 7^-/2_1$	100	100(4)
0.688	$7^-/2_4 \rightarrow 7^-/2_2$	7.1	
	$7^-/2_4 \rightarrow 5^-/2_2$	38.8	
	$7^-/2_4 \rightarrow 9^-/2_2$	75.1	
	$7^-/2_4 \rightarrow 9^-/2_1$	100.0	9(4)
	$7^-/2_4 \rightarrow 5^-/2_1$	41.7	
	$7^-/2_4 \rightarrow 3^-/2_1$	40.3	22(9)
	$7^-/2_4 \rightarrow 7^-/2_1$	38.3	100(7)
0.837	$13^-/2_1 \rightarrow 11^-/2_1$	0.1	
	$13^-/2_1 \rightarrow 9^-/2_2$	0.1	
	$13^-/2_1 \rightarrow 9^-/2_1$	100	100(14)
1.041	$13^-/2_2 \rightarrow 13^-/2_1$	63.2	$\approx 50$
	$13^-/2_2 \rightarrow 11^-/2_1$	1.3	100(50)
	$13^-/2_2 \rightarrow 9^-/2_2$	0.0	
	$13^-/2_2 \rightarrow 9^-/2_1$	100	100(50)
1.273	$15^-/2_1 \rightarrow 13^-/2_2$	17.2	
	$15^-/2_1 \rightarrow 13^-/2_1$	0.3	
	$15^-/2_1 \rightarrow 11^-/2_1$	100	100(24)

TABLE X: Experimental and calculated B(E2) (in unit  $e^2b^2$ ) and B(M1) (in unit  $\mu_N^2$ ), the Quadrupole moment and Magnetic moment of ground state and low-lying states listed in last lines for  $^{151,153}\text{Ho}$  isotopes.

$J_i^- \rightarrow J_f^-$	$^{151}\text{Ho}$		$^{153}\text{Ho}$		$^{153}\text{Ho}$		$^{153}\text{Ho}$	
	B(E2)	EXP.	B(M1)	EXP.	B(E2)	EXP.	B(M1)	EXP.
$9^-/2_1 \rightarrow 11^-/2_1$	0.0612		0.0216		0.0628		0.0684	
$7^-/2_1 \rightarrow 11^-/2_1$	0.0645				0.0596			
$7^-/2_1 \rightarrow 9^-/2_1$	0.0150		0.2398		0.0204		0.2956	
$15^-/2_1 \rightarrow 11^-/2_1$	0.0659				0.0643			
$13^-/2_1 \rightarrow 11^-/2_1$	0.0697		0.0083		0.0717		0.0013	
$13^-/2_1 \rightarrow 9^-/2_1$	0.0082				0.0076			
$13^-/2_1 \rightarrow 15^-/2_1$	0.0027		0.0887		0.0061		0.0274	
$11^-/2_2 \rightarrow 11^-/2_1$	0.0664		0.0005		0.0650		0.0006	
$11^-/2_2 \rightarrow 9^-/2_1$	0.0039		0.1046		0.0006		0.0103	
$11^-/2_2 \rightarrow 13^-/2_1$	0.0004		0.0942		0.0015		0.0153	
$11^-/2_2 \rightarrow 15^-/2_1$	0.0039				0.0036			
$5^-/2_1 \rightarrow 7^-/2_1$	0.0865		0.0041		0.0850		0.0133	
$5^-/2_1 \rightarrow 9^-/2_1$	0.0363				0.0345			
$7^-/2_2 \rightarrow 7^-/2_1$	0.0449		0.0007		0.0290		0.0002	
$7^-/2_2 \rightarrow 5^-/2_1$	0.0080		0.4656		0.0093		0.7639	
$3^-/2_1 \rightarrow 7^-/2_1$	0.1238				0.1093			
$3^-/2_1 \rightarrow 7^-/2_2$	0.0249				0.0182			
$13^-/2_2 \rightarrow 11^-/2_2$	0.0071		0.0019		0.0005		0.0022	
$13^-/2_2 \rightarrow 13^-/2_1$	0.0131		0.0018		0.0046		0.0306	
$9^-/2_2 \rightarrow 7^-/2_2$	0.0015		0.4275		0.0010		0.1388	
$9^-/2_2 \rightarrow 9^-/2_1$	0.0625		0.0035		0.0713		0.0077	
$11^-/2_1$	-0.2858		6.9255		-0.2303	-1.1(5)	6.8612	6.81
$9^-/2_1$	-0.0546		5.9162		-0.0359		5.9166	
$7^-/2_1$	-0.2761		5.4478		-0.2538		5.7557	
$15^-/2_1$	-0.4559		8.2781		-0.4735		7.9279	
$13^-/2_1$	-0.2215		7.6754		-0.1816		7.7220	
$11^-/2_2$	-0.0582		6.7618		-0.0271		6.7609	
$7^-/2_2$	0.1773		4.5124		0.2187		4.6364	
$5^-/2_1$	0.1045		3.7040		0.1267		4.0168	
$3^-/2_1$	-0.1572		3.1244		-0.1507		3.8207	

TABLE XI: Experimental and calculated B(E2) (in unit  $e^2b^2$ ) and B(M1) (in unit  $\mu_N^2$ ), the Quadrupole moment and Magnetic moment of ground state and low-lying states listed in last lines for  $^{151,153}\text{Dy}$  isotopes.

$J_i^- \rightarrow J_f^-$	$^{151}\text{Dy}$				$^{153}\text{Dy}$			
	B(E2)		B(M1)		B(E2)		B(M1)	
	IBFM-2	EXP.	IBFM-2	EXP.	IBFM-2	EXP.	IBFM-2	EXP.
$3^-/2_1 \rightarrow 7^-/2_1$	0.1173				0.0389	0.9135(728)		
$9^-/2_1 \rightarrow 7^-/2_1$	0.0079		0.0008		0.0019		0.0002	
$11^-/2_1 \rightarrow 7^-/2_1$	0.1022				0.0364			
$5^-/2_1 \rightarrow 7^-/2_1$	0.0738		0.1245		0.0470	>0.0534	0.0016	
$11^-/2_1 \rightarrow 9^-/2_1$	0.0009		0.0668		0.0008		0.0128	
$5^-/2_1 \rightarrow 3^-/2_1$	0.0140		0.6252		0.0001		0.0910	
$5^-/2_1 \rightarrow 9^-/2_1$	0.0050				0.0221			
$9^-/2_2 \rightarrow 7^-/2_1$	0.0640		0.0417		0.0533		0.0019	
$7^-/2_2 \rightarrow 7^-/2_1$	0.0671		0.0166		0.0147		0.0051	
$7^-/2_2 \rightarrow 5^-/2_1$	0.0094		0.7565		0.0036		0.0778	
$7^-/2_2 \rightarrow 9^-/2_1$	0.0001		0.0384		0.0002		0.0014	
$7^-/2_2 \rightarrow 9^-/2_2$	0.0002		0.7781		0.0012		0.0915	
$9^-/2_2 \rightarrow 9^-/2_1$	0.0028		0.0005		0.0022		0.0016	
$5^-/2_2 \rightarrow 7^-/2_1$	0.0004		0.0335		0.0149		0.0153	
$5^-/2_2 \rightarrow 7^-/2_2$	0.0010		0.0040		0.0059		0.0065	
$5^-/2_2 \rightarrow 3^-/2_1$	0.0048		0.0001		0.0063		0.0170	
$11^-/2_2 \rightarrow 7^-/2_2$	0.0028				0.0015			
$11^-/2_2 \rightarrow 9^-/2_1$	0.0731		0.0554		0.0014		0.0043	
$11^-/2_2 \rightarrow 9^-/2_2$	0.0016		0.0006		0.0018		0.1213	
$13^-/2_1 \rightarrow 9^-/2_1$	0.1174				0.1030			
$13^-/2_1 \rightarrow 11^-/2_1$	0.0047		0.0003		0.0000		0.0006	
$15^-/2_1 \rightarrow 13^-/2_1$	0.0012		0.1076		0.0001		0.0001	
$7^-/2_1$	-0.3868	-0.30(5)	-0.8439	-0.945(7)	-0.1410	-0.02(5)	-0.8907	-0.782(6)
$9^-/2_1$	-0.6378		0.9640		-0.6726		0.9553	
$3^-/2_1$	-0.2672		-1.7209		-0.2167		-1.2199	
$11^-/2_1$	-0.6098		1.0877		-0.3413		0.4119	
$5^-/2_1$	-0.0568		-0.6930		-0.0712		-0.6369	
$9^-/2_2$	-0.3249		0.4675		-0.1749		-0.1302	
$7^-/2_2$	-0.0702		-0.0038		-0.3029		0.1622	
$5^-/2_2$	-0.5281		-0.2779		-0.1388		-0.2006	

TABLE XII: Comparison of  $\log_{10}ft$  values in the decays  $^{151}\text{Ho} \rightarrow ^{151}\text{Dy}$  and  $^{153}\text{Ho} \rightarrow ^{153}\text{Dy}$ , the order of states corresponding to IBFM-2 calculation.

$^{151}\text{Ho} \rightarrow ^{151}\text{Dy}$				$^{153}\text{Ho} \rightarrow ^{153}\text{Dy}$			
odd-p	odd-n	log ft	Exp.	odd-p	odd-n	log ft	Exp.
$11^-/2_1$	$\rightarrow 13^-/2_1$	7.260	6.200	$11^-/2_1$	$\rightarrow 13^-/2_1$	7.231	6.300
$11^-/2_1$	$\rightarrow 13^-/2_2$	8.440		$11^-/2_1$	$\rightarrow 13^-/2_2$	7.793	
$11^-/2_1$	$\rightarrow 13^-/2_3$	8.907		$11^-/2_1$	$\rightarrow 13^-/2_3$	9.456	6.200
$11^-/2_1$	$\rightarrow 13^-/2_4$	9.174		$11^-/2_1$	$\rightarrow 13^-/2_4$	10.228	
$11^-/2_1$	$\rightarrow 13^-/2_5$	8.807		$11^-/2_1$	$\rightarrow 13^-/2_5$	8.515	
$11^-/2_1$	$\rightarrow 11^-/2_1$	8.019		$11^-/2_1$	$\rightarrow 11^-/2_1$	7.961	6.000
$11^-/2_1$	$\rightarrow 11^-/2_2$	5.429	5.500	$11^-/2_1$	$\rightarrow 11^-/2_2$	7.210	
$11^-/2_1$	$\rightarrow 11^-/2_3$	6.877		$11^-/2_1$	$\rightarrow 11^-/2_3$	5.366	
$11^-/2_1$	$\rightarrow 11^-/2_4$	7.742		$11^-/2_1$	$\rightarrow 11^-/2_4$	9.596	
$11^-/2_1$	$\rightarrow 11^-/2_5$	7.195		$11^-/2_1$	$\rightarrow 11^-/2_5$	6.707	6.300
$11^-/2_1$	$\rightarrow 11^-/2_6$	6.753		$11^-/2_1$	$\rightarrow 11^-/2_6$	7.358	6.300
$11^-/2_1$	$\rightarrow 9^-/2_1$	3.511	4.600	$11^-/2_1$	$\rightarrow 9^-/2_1$	3.612	4.700
$11^-/2_1$	$\rightarrow 9^-/2_2$	4.759	5.800	$11^-/2_1$	$\rightarrow 9^-/2_2$	7.175	6.500
$11^-/2_1$	$\rightarrow 9^-/2_3$	5.208	5.100	$11^-/2_1$	$\rightarrow 9^-/2_3$	6.443	
$11^-/2_1$	$\rightarrow 9^-/2_4$	7.320		$11^-/2_1$	$\rightarrow 9^-/2_4$	4.889	
$11^-/2_1$	$\rightarrow 9^-/2_5$	5.506		$11^-/2_1$	$\rightarrow 9^-/2_5$	6.570	